

Uncertainty Estimation on Sequential Labeling via Uncertainty Transmission

Jianfeng He[†], Linlin Yu[‡], Shuo Lei[†], Chang-Tien Lu[†], Feng Chen[‡]

[†]Department of Computer Science, Virginia Tech, Falls Church, VA, USA

[‡]Department of Computer Science, The University of Texas at Dallas, Richardson, TX, USA

[†]{jianfenghe, slei, ctlu}@vt.edu,

[‡]{Feng.Chen, Linlin.Yu}@utdallas.edu

Abstract

Sequential labeling is a task predicting labels for each token in a sequence, such as Named Entity Recognition (NER). NER tasks aim to extract entities and predict their labels given a text, which is important in information extraction. Although previous works have shown great progress in improving NER performance, uncertainty estimation on NER (UE-NER) is still underexplored but essential. This work focuses on UE-NER, which aims to estimate uncertainty scores for the NER predictions. Previous uncertainty estimation models often overlook two unique characteristics of NER: the connection between entities (i.e., one entity embedding is learned based on the other ones) and wrong span cases in the entity extraction subtask. Therefore, we propose a Sequential Labeling Posterior Network (SLPN) to estimate uncertainty scores for the extracted entities, considering uncertainty transmitted from other tokens. Moreover, we have defined an evaluation strategy to address the specificity of wrong-span cases. Our SLPN has achieved significant improvements on three datasets, such as a 5.54-point improvement in AUPR on the MIT-Restaurant dataset. Our code is available at https://github.com/he159ok/UncSeqLabeling_SLPN.

1 Introduction

Named entity recognition (NER) is a popular task in the information extraction domain (Lample et al., 2016), which involves two steps, detecting entity spans and predicting the entity labels. In many information extraction scenarios, there are significant consequences for relying on inaccurate NER predictions. For example, extracting an inaccurate time can lead to erroneous policy analysis, or misclassifying a person’s name for a time can result in a privacy breach. Therefore, it is crucial to determine whether we can trust the NER predictions or not. As a result, our goal is to enhance Uncer-

tainty Estimation in NER (UE-NER), which aims to quantify prediction confidence in NER tasks.

The NER task differs from general classification (e.g., text classification (Minaee et al., 2021) in two key ways, making previous uncertainty estimation models suboptimal for UE-NER.

First, the predicted entity labels in the NER task are directly dependent on the token embeddings, and uncertainty transmission between token embeddings is unique in NER. Concretely, given an example text “Barack Obama was born in Honolulu, Hawaii,” the entity label “person” applies to “Barack Obama.” The embedding of the token “Obama” is obtained by accumulating its own embedding and embeddings from other tokens in Recurrent Neural Network (Medsker and Jain, 2001) and transformer (Vaswani et al., 2017). Consequently, if a token embedding has higher uncertainty, the other token embedding will have more transmitted uncertainty from the token. Since token embeddings directly affect token labels and further affect entity labels, high uncertainty in a token embedding will result in a predicted entity label with high uncertainty. Therefore, in the context of UE-NER, a token uncertainty in UE-NER consists the individual token uncertainty and the uncertainty transmitted from other tokens.

However, the current uncertainty estimation methods ignore the uncertainty transmission between tokens. Especially, current uncertainty estimation methods can be classified into two main categories: parameter-distribution-based methods, such as Bayesian Neural Networks (BNN)(Osawa et al., 2019; Maddox et al., 2019), which learns a distribution over the model parameters; and sample-distribution-based methods, which calculate uncertainty scores based on the distribution of training samples (Charpentier et al., 2020; He et al., 2020; Park et al., 2018). These methods primarily focus on image or text classification, where correlations between different images or texts are weak or lim-

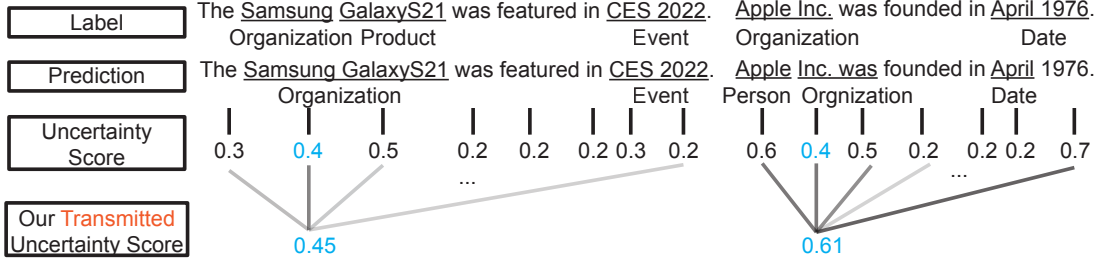


Figure 1: In this example, though the tokens “Samsung” and “Inc.” both have the same uncertainty score of 0.4, the context in the right case exhibits higher uncertainty. This suggests that “Inc.” should be considered more uncertain than “Samsung.” Therefore, we propose transmitting the predicted uncertainty from other tokens to a given token.

ited. Consequently, they overlook the uncertainty transmission inherent in sequential labeling. Since sequential labeling plays a pivotal role in Natural Language Processing (NLP), with NER as a representative example, it is imperative for us to address UE-NER by considering uncertainty transmission, shown as Figure 1.

The second characteristic of NER tasks is that they involve an additional step, entity extraction, besides entity classification. In contrast to previous text classification tasks (Minaee et al., 2021), which focus solely on sample classification, NER tasks require the additional task of extracting entity spans, such as locating “Barack Obama.” However, entity span extraction may predict entities with wrong span (WS), such as predicting “Obama was” as an entity. These WS entities lack ground truth entity labels and evaluating uncertainty estimation requires ground truth labels, thus these entities cannot be used for evaluating uncertainty estimation. Therefore, we require an innovative approach to evaluate a UE-NER model that takes into account these WS entities.

To address the first issue, we propose a Sequential Labeling Posterior Network (SLPN) for transmitting uncertainty. This network is built upon an evidential neural network framework (Charpentier et al., 2020) with a novel design to transmit uncertainty from other tokens. For the second issue, we categorize the ground truth entities and predicted entities into three groups: unique entities in the ground truth, unique entities in the prediction, and shared entities between the ground truth and prediction. We, then, treat WS entity detection as a separate subtask, in addition to out-of-domain (OOD) detection, which is a common task used to evaluate uncertainty estimation (Zhao et al., 2020). The WS and OOD detections use different combinations of the three-group entities. Furthermore,

we evaluate the performance of a UE-NER model by computing a weighted sum of WS entity detection and OOD detection performance, providing a comprehensive assessment of the UE-NER model. Our contributions are as follows.

- Since each token embedding is influenced by other tokens within a given text, and token embedding directly affects the uncertainty of predicted entity labels, we propose a novel method to transmit uncertainty between tokens using a revised self-attention. To the best of our knowledge, we are the first to consider uncertainty transmission in UE-NER.
- Because of the existence of WS entities in the NER task, we have found that traditional evaluation methods for uncertainty estimation are inapplicable in UE-NER. Therefore, we propose a novel uncertainty estimation evaluation to evaluate both OOD and WS detection tasks.

2 Related Work

Named Entity Recognition. Named Entity Recognition (NER) is a task focused on extracting and classifying entities within text. It serves as a prominent example of sequential labeling, where each token in a sequence is assigned a label. Various techniques have been employed for NER, including Recursive Neural Networks (e.g., LSTM (Hamerton, 2003)), pretrained transformer models (e.g., BERT (Devlin et al., 2018)). In some cases, Conditional Random Fields (CRF) are incorporated into token encoders, such as LSTM+CRF (Lample et al., 2016), to enhance performance.

Further, recent experiments have explored the use of Large Language Models (LLMs) for NER. An LLM-based approach treats NER as a generative task, with each turn generating one category of entities (Wang et al., 2023b). However, it is no-

ticeable that Wang et al. (2023b) found that GPT3-based NER solutions (Floridi and Chiriatti, 2020) did not outperform pretrained transformer based method. Since both pretrained transformer-based methods and LLMs are built on transformer architectures (Vaswani et al., 2017) and pretrained transformer-based methods take NER as sequential generation rather than sequential labeling, as well as perform better than GPT-3 on the NER task, our research focuses on UE-NER using pretrained-transformer-based methods.

Uncertainty estimation on natural language processing. Generally, for the usage of uncertainty estimation on training data, the uncertainty score helps with sample selection in active learning (Wang et al., 2021). For usage on the testing data, uncertainty estimation mainly serves two tasks: *OOD detection* (Hart et al., 2023), where the testing samples include OOD samples, and the task aims to identify these OOD samples; and *misclassified result detection*: where testing samples are in-domain (Zhang et al., 2019; He et al., 2020; Hu and Khan, 2021). Our work specifically focuses on OOD detection in the testing samples.

In the NER domain, Nguyen et al. (2021); Chang et al. (2020); Liu et al. (2022) estimated uncertainty scores on unlabeled training data for active learning. Vazhentsev et al. (2022) were the first to apply uncertainty estimation to address misclassification in NER testing data using techniques like dropout (Gal and Ghahramani, 2016) and deterministic uncertainty estimation methods (e.g., Gaussian process (Liu et al., 2020)). Additionally, on the testing samples, Zhang et al. (2023) were the first to apply uncertainty estimation to detect OOD instances in NER testing data. Compared to Zhang et al. (2023), who assigned different weights to different tokens, our work focuses on the transmission of uncertainty from other tokens to a specific token.

3 UE-NER Task Setting

Before we introduce UE-NER, we first introduce NER tasks, which is a representative sequential labeling task. Given a text $\mathbf{X} = [\mathbf{x}_1, \mathbf{x}_2, \dots, \mathbf{x}_n]$ with n tokens, where $\mathbf{x}_i \in \mathbb{R}^{h \times 1}$ is an embedding of a token, NER task aims at learning a NER model predicting their token labels. Then, the entities are extracted by the token labels based on the BIOES mechanism (Chiu and Nichols, 2016) (e.g., “Brack” with B-PER label, and “Obama” with I-PER label). Moreover, the extracted entities are classified by

merging the entity tokens. For example, “Brack Obama” is categorized as a Person because these two tokens are categorized as the beginning and intermediate of the person label.

For the UE-NER task, we aim to learn a UE-NER model Φ to predict the confidence of each predicted token label. We apply Φ for OOD detection, which is a common task to evaluate uncertainty estimation (Zhao et al., 2020). Concretely, the training data and validation data for Φ are the in-domain (ID) text without OOD entities. The testing data of Φ includes both ID text and OOD text, where OOD text has both ID and OOD entities. A better Φ should detect more OOD entities in the testing set and have better NER performance.

4 Preliminary: Posterior Network

The parameter-distribution-based uncertainty estimation method is usually implemented via ensemble sampling (Gal and Ghahramani, 2016) and thus requires multiple forward passes to estimate uncertainty, which is time-consuming. In contrast, Evidential Deep Learning (EDL) (Sensoy et al., 2018) is a representative sample-distribution-based uncertainty estimation method and is implemented via a deterministic model, thus requiring only one forward pass to estimate uncertainty. Due to its efficiency, we choose EDL.

In EDL, considering the classification task and given the input vector \mathbf{X} , the class prediction $y \in [c]$ for an input sample follows a categorical distribution with c classes. The categorical distribution naturally follows a Dirichlet distribution, i.e.

$$y \sim \text{Cat}(\mathbf{p}), \quad \mathbf{p} \sim \text{Dir}(\boldsymbol{\alpha}) \quad (1)$$

The expected class probability $\bar{\mathbf{p}}$ is calculated as below,

$$\alpha_0 = \sum_{k=1}^c \alpha_k, \quad \bar{\mathbf{p}} = \frac{\boldsymbol{\alpha}}{\alpha_0} \quad (2)$$

where $\text{Dir}(\boldsymbol{\alpha})$ is an approximation of the posterior distribution of class probabilities, conditioned on the input feature vector. The concentrate parameters $\boldsymbol{\alpha} = [\alpha_1, \alpha_2, \dots, \alpha_c]$ can be interpreted as the evidence for the given example belonging to the corresponding class (Jang, 2018). The evidence is the count of pseudo support from training samples.

As a representative model of EDL, Posterior Network (PN) (Charpentier et al., 2020) is originally designed for image classification and involves two main steps. First, a feature encoder maps the raw

features into a low-dimensional latent space. Second, a normalizing flow such as Radial (Rezende and Mohamed, 2015) is used to estimate class-wise density on the latent space, which is proportional to the class-wise evidence. Essentially, a greater density for a particular class implies stronger evidence belonging to this class for the given example.

PN is trained with the sum of two loss \mathcal{L}^{UCE} and \mathcal{L}^{ER} for N training samples as below,

$$\mathcal{L}^{\text{UCE}} = \frac{1}{N} \sum_{i=1}^N \mathbb{E}_{\mathbf{p}_i \sim \text{Dir}(\mathbf{p}_i | \boldsymbol{\alpha}_i)} [\text{CE}(\mathbf{p}_i, y_i)] \quad (3)$$

$$\mathcal{L}^{\text{ER}} = -\frac{1}{N} \sum_{i=1}^N \mathbb{H}(\text{Dir}(\mathbf{p}_i | \boldsymbol{\alpha}_i)) \quad (4)$$

where the Uncertainty Cross Entropy (UCE) loss \mathcal{L}^{UCE} encourages high evidence for the ground-truth category and entropy regularization \mathcal{L}^{ER} encourages a smooth Dirichlet distribution.

5 Model

We choose PN as it does not require OOD data during training. In contrast, Prior Network (Malinin and Gales, 2018), another representative EDL method, necessitates OOD data in training. Furthermore, even if OOD data is available, it may not cover all possible OOD scenarios. Thus, we opt for uncertainty transmission based on PN.

5.1 Our Token-Level Posterior Network

The PN, originally for image classification, is applied to NER for the first time to our knowledge. To better apply PN in NER, we first analyze the difference between tokens and samples (e.g., images). Concretely, tokens can be selected from specific sets, allowing for the calculation of token-level categorical distributions. In contrast, for samples, the vast and continuous potential space of unique samples makes it impractical to compute categorical distributions for every possible sample.

To apply PN into UE-NER and consider the above difference, we propose token-level PN, where we propose to calculate a unique categorical distribution for each token, rather than computing a single shared categorical distribution for all samples. This is because each token exhibits distinct semantic characteristics (e.g., “Paris” is more likely to represent a location than “August”), and thus needs individual categorical distributions. Concretely, a categorical distribution $\text{Cat}(\mathbf{p}_i)$ of i -th token in a text is the total occurrence of i -th

token in each of c classes given a training set. For example, the token “Apple” in the training data has 200 and 800 occurrences for the organization and food classes respectively, then “Apple” has categorical distribution as $[0, \dots, 0.2, \dots, 0.8, 0\dots] \in \mathbb{R}^c$.

Then, since the classification is usually taken as a multinomial distribution, we can represent the classification as a posterior distribution as below,

$$\mathbb{P}(\mathbf{p}_i | y_i) \propto \mathbb{P}(y_i | \mathbf{p}_i) \times \mathbb{P}(\mathbf{p}_i) \quad (5)$$

we represent its prior distribution by a Dirichlet distribution $\mathbb{P}(\mathbf{p}_i) = \text{Dir}(\boldsymbol{\beta}^{\text{prior}})$, where $\boldsymbol{\beta}^{\text{prior}}$ is the parameter of the prior Dirichlet distribution. In practice, we set $\boldsymbol{\beta}^{\text{prior}} = \mathbf{1}$ for a flat equiprobable prior when the model brings no initial evidence. Due to the conjugate prior property, the posterior distribution can also be represented by a Dirichlet distribution: $\mathbb{P}(\mathbf{p}_i | y_i) = \text{Dir}(\boldsymbol{\beta}^{\text{prior}} + \boldsymbol{\beta}_i^{\text{post}})$. The $\boldsymbol{\beta}_i^{\text{post}}$ is taken as the evidence count for i -th token. To learn $\boldsymbol{\beta}_i^{\text{post}}$, PN firstly projects i -th token embedding \mathbf{x}_i to a low-dimensional latent vector $\mathbf{z}_i = f(\mathbf{x}_i)$. Then, PN learns a normalized probability density $\mathbb{P}(\mathbf{z}_i | k; \theta)$ per class on this latent space. PN then counts the evidence for k -th class at \mathbf{z}_i as below:

$$\boldsymbol{\beta}_{i,(k)}^{\text{post}} = N \times \mathbb{P}(\mathbf{z}_i | k; \theta) \times \mathbb{P}(k_i) \quad (6)$$

where $\mathbb{P}(k_i)$ is the probability that i -th token belongs to k -th class, extracted from $\text{Cat}(\mathbf{p}_i)$. And $\boldsymbol{\beta}_i^{\text{post}} \in \mathbb{R}^c = [\beta_{i,(1)}^{\text{post}}, \beta_{i,(2)}^{\text{post}}, \dots, \beta_{i,(c)}^{\text{post}}]$. The $\boldsymbol{\beta}_i^{\text{post}}$ can be understood as the evidence distribution for i -th tokens. For a text with l tokens, we can concatenate all l tokens’ evidence distribution vector $\boldsymbol{\beta}^{\text{post}}$ and have $\boldsymbol{\beta}^{\text{post},t} \in \mathbb{R}^{l \times c}$.

Difference to original posterior network. Compared to the original sample-level posterior network (Charpentier et al., 2020), which operates at the sample level, our token-level PN differs in two key ways: (1) We use a token-level categorical distribution instead of a sample-level categorical distribution shared among all samples. (2) We concatenate the $\boldsymbol{\beta}^{\text{post}}$ values for each of the l tokens to create a new matrix $\boldsymbol{\beta}^{\text{post},t} \in \mathbb{R}^{l \times c}$ to facilitate uncertainty transmission in Sec. 5.2, a step not required in the original PN.

5.2 Our SLPN

Though the token-level PN counts the evidence given a token, it ignores the relation between tokens. Shown as Fig. 1, imagine that Token A comes from Text A, and Token B comes from Text B.

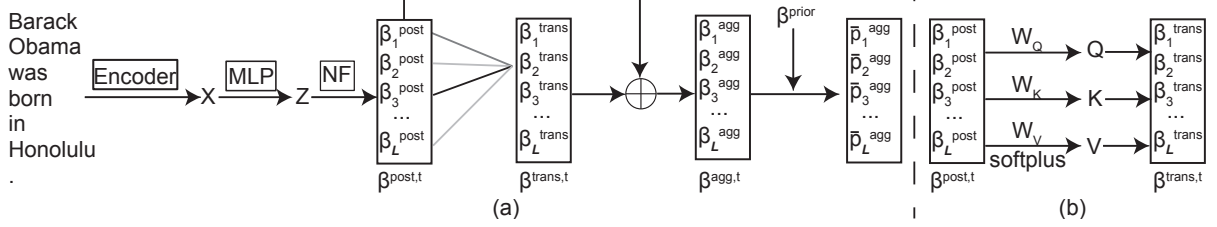


Figure 2: (a) A diagram of our SLPN model illustrates how we achieve uncertainty transmission through a revised self-attention mechanism applied to all tokens. Specifically, the SLPN model begins by generating a text embedding matrix \mathbf{X} with l rows, corresponding to a text containing l tokens. Next, an MLP model projects \mathbf{X} into a latent embedding matrix \mathbf{Z} also with l rows. This \mathbf{Z} matrix is used to compute $\beta^{post,t} \in \mathbb{R}^{l \times c}$ through a normalizing flow (NF) operation. Each row of $\beta^{post,t}$ represents the evidence count from the token's self-view, directly influencing the uncertainty of each token's prediction. In contrast to previous research, our approach includes the transmission of uncertainty from all tokens within the text to obtain the transmitted uncertainty $\beta^{trans,t}$. Finally, we combine the sum of $\beta^{post,t}$ and $\beta^{trans,t}$ to generate the semantic matrix $\mathbf{p}^{agg} \in \mathbb{R}^{l \times c}$, representing the semantics of the l tokens. (b) Revised self-attention mechanism.

Token A and Token B have the same predicted uncertainty in terms of token label when only considering the token itself. If the other tokens in Text A have more uncertainty than other tokens in Text B, then in this case, Token A should be more uncertain than Token B due to the impact of other tokens. Thus, we propose a Sequential Labeling Posterior Network (SLPN), which takes the uncertainty impact transmitted from other tokens into consideration.

Concretely, shown as Figure 2(a), a token embedding has accumulated all other token embeddings by the Bidirectional RNN (Huang et al., 2015) or transformer (Vaswani et al., 2017). As a result, token uncertainty should comprise two components: uncertainty originating from the token itself and uncertainty transmitted from other tokens. Since the uncertainty in EDL depends on the evidence count vector $\beta \in \mathbb{R}^c$, we can represent the aggregated uncertainty $\beta_i^{agg} \in \mathbb{R}^c$ for i -th token as below,

$$\beta_i^{agg} = \beta_i^{post} + \beta_i^{trans} \quad (7)$$

where β_i^{post} is the uncertainty coming from the token itself and $\beta_i^{trans} \in \mathbb{R}^c$ is the transmitted uncertainty from all tokens to i -th token in the text. The calculation of β_i^{post} is described in Sec. 5.1.

Calculation of impact transmission weight β_i^{trans} . Since β_i^{trans} accumulates all the impact from all tokens in a text, we calculate β_i^{trans} in a way motivated by self-attention (Vaswani et al., 2017). Concretely, we have three projector matrices $W_Q \in \mathbb{R}^{c \times p}$, $W_K \in \mathbb{R}^{c \times p}$ and $W_V \in \mathbb{R}^{c \times c}$ to get the query $Q \in \mathbb{R}^{l \times p}$, key $K \in \mathbb{R}^{l \times p}$ and value

$V \in \mathbb{R}^{l \times c}$ as below,

$$\begin{aligned} Q &= \beta^{post,t} W_Q, K = \beta^{post,t} W_K \\ V &= \text{softplus}(\beta^{post,t} W_V) \end{aligned} \quad (8)$$

where p is a pre-set dimension. Different from self-attention, we keep the shape of the V the same as $\beta^{post,t}$, because the $\beta^{post,t}$ has the evidence distribution and we want to avoid multiple projections that might lose the evidence distribution. Besides, we apply the *softplus* activation function (Sun et al., 2020) to make sure the value of V is always greater than 0. We require evidence greater than 0 because EDL is an evidence acquisition process where each training sample adds support to learn higher order evidence distribution, and thus evidence can only be increased and not decreased (Amini et al., 2020; Wang et al., 2023a). Then, we get the transmitted uncertainty $\beta^{trans,t} \in \mathbb{R}^{l \times c}$ as below,

$$\beta^{trans,t} = \text{softmax}\left(\frac{QK^T}{\gamma}\right)V \quad (9)$$

where γ is the hyperparameter to rescale the weight to avoid gradient explosion. More explanation is given in Sec. A.1.1.

Training Loss. Once we have obtained β^{agg} using Eq. 7, we train our SLPN model via below loss.

$$\begin{aligned} L &= \frac{1}{N} \sum_{i=1}^N \mathbb{E}_{\mathbf{p}_i^{agg} \sim \text{Dir}(\mathbf{p}_i^{agg} | \alpha_i^{agg})} [\text{CE}(\mathbf{p}_i^{agg}, \mathbf{y}_i)] \\ &\quad - \lambda \frac{1}{N} \sum_{i=1}^N \mathbb{H}(\text{Dir}(\mathbf{p}_i^{agg} | \alpha_i^{agg})) \end{aligned} \quad (10)$$

where $\alpha_i^{agg} = \beta_i^{agg} + \beta^{prior}$ and the expected aggregated class probability of the i -th token calculated based on β_j^{agg} is below,

$$\bar{\mathbf{p}}_i^{agg} = \frac{\beta_i^{agg} + \beta^{prior}}{\sum_{k=1}^c (\beta_{i,(k)}^{agg} + \beta_k^{prior})} \quad (11)$$

where $\beta^{prior} \in \mathbb{R}^c$ is the vector with all default values as 1. As a result, the first item in Eq. 10 is the UCE loss in the token level like Eq. 3, and the second item in Eq. 10 is a regularization encouraging a smooth Dirichlet distribution for each token.

6 Experiments

6.1 Experimental Setup

6.1.1 Dataset Setup

Dataset. We apply three public datasets: (1) MIT-Restaurant (**MIT-Res**) dataset is in the restaurant domain with a total of 9181 texts with 8 semantic classes, excluding the “O” class. (2) Movie-Simple (**Mov-Sim**) dataset is in the movie domain with a total of 12,218 texts with 12 semantic classes, excluding the “O” class. (3) Movie-Complex (**Mov-Com**) dataset is also in the movie domain with a total of 9769 texts with 12 semantic classes, excluding the “O” class. These three datasets are provided in a common NER framework, Flair (Akbik et al., 2019). The criteria of the dataset choice are detailed in Sec. A.2.1.

OOD entity construction & data split. Our OOD entities are constructed using the leave-out method. Specifically, given an NER dataset with different kinds of entity labels, we count the number of entities for each label. Subsequently, we select and leave out m labels with the lowest entity counts. This choice is made to ensure that there is a sufficient amount of data available for training and validation purposes. After applying the leave-out method, we represent the remaining labels as S^{in} , which includes c labels, and the corresponding text sets as D^{in} . Similarly, we represent the labels that were left out as S^{out} , which contains m OOD labels, and the corresponding text sets as D^{out} . All text samples in D^{in} are labeled only with entities from S^{in} and do not include any labels from S^{out} . Conversely, all text samples in D^{out} must contain at least one label from S^{out} .

We use 80% of the samples from D^{in} for training and 10% for validation. Our testing set comprises the remaining 10% of the samples from D^{in} and all samples from D^{out} .

6.1.2 Evaluation on OOD Detection

Our uncertainty estimation is evaluated via OOD detection at the entity level (e.g., “New York” is an entity with the label “LOC”). The reason for using entity-level evaluation is detailed in Sec. A.2.2.

Wrong-span (WS) entities. However, OOD detection evaluation in the NER task faces challenges related to wrong-span (WS) entities. Unlike traditional image or text sample-level classification, NER tasks require the prediction of entity spans first. An entity may span one or several tokens. There are the following three cases related to OOD detection: (1) the predicted OOD entity exactly matches a true OOD entity; (2) the predicted OOD entity partially matches a true OOD entity on some tokens; (3) the predicted OOD entity does not match a true OOD entity on any tokens. We denote the second and third cases as “WS”.

Three kinds of entities. Then, because these WS entities do not have ground truth ID/OOD labels, these WS entities are inapplicable for OOD detection evaluation. Besides, we are also interested in whether our UE-NER model can handle WS entity prediction as well. As a result, we aim to evaluate our UE-NER model Φ by both OOD detection and WS entity predictions. Because the entities applicable for evaluating WS entity prediction might be inapplicable for evaluating OOD detection, we divide the ground truth entities and predicted entities into three parts: (1) Unique predicted entities \hat{e}^p , which do not exist in the ground truth and thus are the WS entities; (2) Unique ground-truth entities \hat{e}^g , which are the entities that do not appear in the predicted entities; (3) Shared entities e^s , which are the predicted entities matching the ground truth.

Then, all predicted entities, including shared entities, are represented as $e^p = e^s + \hat{e}^p$. Original ground-truth entities (without “WS” labels) are denoted as $e^{og} = e^s + \hat{e}^g$, and new ground-truth entities (including “WS” labels) are represented as $e^{ng} = e^s + \hat{e}^g + \hat{e}^p$.

Entities applied to OOD or WS detection. For NER OOD detection, the ground-truth labels in OOD detection should be binary, “ID” and “OOD” labels, while NER ground-truth labels have three: “ID”, “OOD” and “WS” labels. As a result, we divide NER OOD detection into two subset for the evaluation. One subset has entities ($e^{og} = e^s + \hat{e}^g$) with “ID” and “OOD” for evaluating NER OOD detection, the other subset has $e^{ng} = e^s + \hat{e}^g + \hat{e}^p$ entities for evaluating WS detection. For OOD

Table 1: The table lists the applied entities for OOD and WS tasks. Recall that original ground-truth entities are $e^{og} = e^s + \hat{e}^g$ (used for OOD detection subtask), new ground-truth entities are $e^{ng} = e^s + \hat{e}^g + \hat{e}^p$ (used for WS detection subtask). The values in the brackets are the possible ground truth label values.

| | e^s | \hat{e}^g | \hat{e}^p |
|-----------------------------|--------------|--------------|------------------|
| Ground-truth entity labels | ID or OOD | ID or OOD | WS |
| OOD detection subtask usage | use (0 or 1) | use (0 or 1) | do not use (N/A) |
| WS detection subtask usage | use (0) | use(0) | use (1) |

Table 2: Uncertainty estimation results MS_{ood+ws} on both OOD & WS tasks, the formula of MS_{ood+ws} is described in Eq. 12. The bold font annotates the best performance among a subregion. This bold font aligns with methodologies employed in similar studies on uncertainty estimation, including those detailed in Table 14 of [Stadler et al. \(2021\)](#) and Table 2 of [Zhao et al. \(2020\)](#).

| Data | Model | weighted AUROC on both OOD & WS task | | | | | weighted AUPR on both OOD & WS task | | | | | F1 |
|---------|--------------------|--------------------------------------|-------|-------|--------------|-------|-------------------------------------|-------|-------|--------------|-------|--------------|
| | | Va. | Dis. | Al. | Ep. | En. | Va. | Dis. | Al. | Ep. | En. | |
| Mov-Sim | Dropout | - | - | 68.66 | 71.09 | 72.11 | - | - | 27.98 | 34.06 | 31.28 | 83.94 |
| | PN | 79.34 | 54.41 | 66.56 | 79.34 | 65.14 | 40.88 | 16.90 | 30.27 | 40.88 | 27.72 | 82.43 |
| | E-NER | 77.58 | 59.05 | 76.82 | 77.58 | 77.61 | 36.40 | 20.44 | 35.72 | 36.40 | 36.05 | 70.63 |
| | SLPN(w/o softplus) | 60.12 | 39.66 | 45.35 | 60.12 | 37.33 | 28.72 | 16.57 | 23.47 | 28.72 | 19.36 | 66.95 |
| | Ours(SLPN) | 78.37 | 54.22 | 64.40 | 78.37 | 62.20 | 47.23 | 16.93 | 30.43 | 47.23 | 26.21 | 83.37 |
| MIT-Res | Dropout | - | - | 61.10 | 65.86 | 63.34 | - | - | 36.66 | 47.90 | 41.15 | 74.60 |
| | PN | 69.77 | 66.62 | 61.99 | 69.77 | 67.03 | 46.56 | 39.33 | 38.71 | 46.56 | 42.03 | 74.37 |
| | E-NER | 67.74 | 67.29 | 65.62 | 67.74 | 67.30 | 41.62 | 40.58 | 39.91 | 41.62 | 40.58 | 69.08 |
| | SLPN(w/o softplus) | 50.78 | 50.05 | 52.48 | 50.78 | 49.92 | 32.97 | 31.62 | 33.43 | 32.97 | 32.37 | 62.16 |
| | Ours(SLPN) | 70.01 | 49.14 | 57.17 | 70.01 | 53.02 | 49.91 | 32.08 | 35.23 | 49.91 | 34.85 | 74.65 |
| Mov-Com | Dropout | - | - | 55.82 | 56.44 | 56.13 | - | - | 17.01 | 18.68 | 17.40 | 72.51 |
| | PN | 72.65 | 68.07 | 71.08 | 72.65 | 69.43 | 28.88 | 22.93 | 27.47 | 28.88 | 25.99 | 70.13 |
| | E-NER | 77.93 | 73.77 | 77.68 | 77.93 | 75.55 | 34.32 | 25.34 | 29.48 | 34.32 | 27.99 | 67.21 |
| | SLPN(w/o softplus) | 60.77 | 54.44 | 57.91 | 60.77 | 55.56 | 25.18 | 20.93 | 24.32 | 25.18 | 22.71 | 66.05 |
| | Ours(SLPN) | 81.31 | 48.52 | 71.18 | 81.31 | 57.11 | 38.47 | 17.50 | 25.53 | 38.47 | 20.70 | 70.97 |

Table 3: Size statistics on the three cases in three datasets.

| Data | Model | e^{ng} | e^s | \hat{e}^p | \hat{e}^g |
|---------|---------------------|----------|-------|-------------|-------------|
| Mov-Sim | Dropout | 4412 | 3055 | 488 | 869 |
| | PN | 4475 | 2974 | 551 | 950 |
| | E-NER | 4847 | 2665 | 923 | 1259 |
| | SLPN (w/o softplus) | 4991 | 2654 | 1067 | 1270 |
| | Ours (SLPN) | 4426 | 3060 | 502 | 864 |
| MIT-Res | Dropout | 7217 | 3793 | 1043 | 2381 |
| | PN | 7187 | 3667 | 1013 | 2507 |
| | E-NER | 7297 | 3456 | 1123 | 2718 |
| | SLPN (w/o softplus) | 7904 | 3646 | 1730 | 2528 |
| | Ours (SLPN) | 7237 | 3872 | 1063 | 2302 |
| Mov-Com | Dropout | 5551 | 3039 | 1019 | 1493 |
| | PN | 5772 | 3004 | 1240 | 1528 |
| | E-NER | 5689 | 2722 | 1157 | 1810 |
| | SLPN (w/o softplus) | 6043 | 2985 | 1511 | 1547 |
| | Ours (SLPN) | 5746 | 3045 | 1214 | 1487 |

detection task, we take “OOD” labels as 1 and “ID” labels as 0. For WS detection, we take “WS” labels as 1, “ID” and “OOD” labels as 0. We list the applied entities of these two cases in Tab. 1.

6.1.3 Experimental Settings

Baselines. Because UE-NER is underexplored, we use three baselines in our experiments: (1) Dropout ([Gal and Ghahramani, 2016](#)), which is an ensemble-based method to approximate BNN. It needs to run multiple times for the uncertainty estimation while our SLPN can get the estimated uncertainty by only running once. (2) PN ([Charpentier et al., 2020](#)), which has been revised into token-level PN for UE-NER task, introduced in

Sec. 5.1. (3) E-NER ([Zhang et al., 2023](#)) learns importance weights via evidence distribution and adds a regularization for increasing learned uncertainty of the wrong prediction.

Ablation Settings. Besides PN, we design SLPN (w/o softplus) for the ablation study. The SLPN (w/o softplus) removes the softplus in Eq. 8.

Uncertainty Metrics. We measure uncertainty estimation performance using five types of uncertainty. Specifically, Dissonance (Dis.) and vacuity (Va.) uncertainties are concepts proposed in the domain of evidential theory ([Sensoy et al., 2018](#)). (1) Dissonance uncertainty refers to conflicting evidence, where the evidence for a particular class is similar to the evidence for other classes. (2) Vacuity uncertainty indicates a lack of evidence, where the evidence for all classes is of very small magnitude ([Lei et al., 2022](#)). Besides, aleatoric (Al.) and epistemic uncertainty (Ep.) are proposed from the probabilistic view. (3) Aleatoric uncertainty arises from the inherent stochastic variability in the data generation process, such as noisy sensor data ([Dong et al., 2022a](#)). (4) Epistemic uncertainty stems from our limited knowledge about the data distribution, like OOD data. Moreover, we also consider (5) uncertainty calculated by entropy. We select the best-performing metric for each method from the five available uncertainty metrics. These

five types of uncertainty are all measured via AUROC and AUPR (Hu and Khan, 2021; Zhao et al., 2020; Malinin and Gales, 2018; Hendrycks and Gimpel, 2016; Dong et al., 2022b; Yu et al., 2023). More details about the five uncertainty metrics are in Sec. A.2.3.

For Tables 2, 4, and 5, we annotate the best performance within a subregion in bold font. This practice aligns with methodologies employed in similar studies on uncertainty estimation, including those detailed in Table 14 of Stadler et al. (2021) and Table 2 of Zhao et al. (2020).

Performance combined OOD and WS detection performance. Because we have OOD detection and WS detection tasks on NER uncertainty estimation, we propose to merge the results of the two tasks. This will enable us to determine which UE-NER model is better. As a result, we merge them by weighting the OOD detection results and WS detection results based on the size ratio between e^s and \hat{e}^p , as shown below.

$$MS_{ood+ws} = \frac{e^s}{e^s + \hat{e}^p} MS_{ood} + \frac{\hat{e}^p}{e^s + \hat{e}^p} MS_{ws} \quad (12)$$

Where MS_{ood+ws} represents the metric score weighted by the respective OOD task metric score MS_{ood} and the WS task metric score MS_{ws} .

6.2 Experimental Results

Our SLPN performs better than the baselines in weighted metric performance, which indicates that transmitted uncertainty from other tokens benefits the model performance. Table 2 shows that our SLPN outperforms the baselines in weighted metric performance, except for AUROC on Movie-Simple. Specifically, our SLPN surpasses the baselines in both AUROC and AUPR on the MIT-Restaurant dataset. For instance, our SLPN improves AUPR by 2.01 points compared to dropout and 3.25 points compared to PN. On the Movie-Simple dataset, the AUPR also indicates that our SLPN performs better than other methods, with an improvement of 6.35 points compared to PN. Although the AUROC on Movie-Simple does not exceed the baselines, the difference from PN is less than 1 point. Plus, on the Movie-Complex dataset, our work also surpasses the baselines, such as a 3.38 points improvement over the E-NER in AUROC. Taken together, these results demonstrate that the transmitted uncertainty from other tokens applied in SLPN benefits the model’s performance.

The entity size distribution of our SLPN is similar to that of the baselines, except E-NER. Table 3 shows that the entity distributions for the three types of entities are similar among dropout, PN, and our SLPN. The relatively greater number of unique predicted entities \hat{e}^p and the lower number of unique ground truth entities \hat{e}^g compared to dropout suggests that our SLPN primarily improves OOD detection rather than WS detection. Consequently, future research can focus on enhancing WS detection or both of these detection tasks.

Additionally, we observe that E-NER has relatively fewer shared entities e^s . We speculate that this could be due to E-NER not demonstrating as powerful NER classification performance as dropout, PN, and our SLPN in these three datasets.

Our SLPN performs better than the baselines in OOD detection performance. Table 4 shows that E-NER performs better than our SLPN in Movie-Simple and MIT-Restaurant datasets, the E-NER sacrifices the NER classification performance. Among Dropout, PN and our SLPN, which have the similar high classification performance, our method performs better in OOD detection performance. For example, on the MIT-Restaurant dataset, our SLPN improves AUROC by 1.63 points compared to PN and 10.87 points compared to Dropout. However, on the Movie-Simple dataset, our SLPN has a difference of less than 1 point compared to PN, but our AUPR surpasses PN by 7.06 points.

Our SLPN performs unsatisfactorily compared to the baselines in WS detection performance. Although our SLPN performs very well in OOD detection, its performance in WS detection in Table 5 is unsatisfactory. However, the sizes of WS entities (\hat{e}^p) are very similar among dropout, PN, and our SLPN on both datasets. For example, the sizes of \hat{e}^p are 1043, 1013, and 1063 for dropout, PN, and our SLPN, respectively. This means our SLPN performs unsatisfactorily in WS detection.

Our SLPN performs close or even better than the dropout in terms of the NER task performance. From Table 5, our NER performance closely matches dropout, differing by less than 1 point in F1 scores on the Movie-Simple dataset. Notably, dropout is an ensemble-based approach known for enhancing model performance. Despite this, our SLPN achieves comparable or superior NER F1 scores, demonstrating its ability to enhance UE-NER performance while preserving the original NER model’s effectiveness.

The activation function softplus is important to

Table 4: Uncertainty estimation results on OOD task. The usage of bold font is the same as Table 2.

| Data | Model | AUROC on OOD task | | | | | AUPR on OOD task | | | | | F1 |
|---------|--------------------|-------------------|-------|-------|--------------|-------|------------------|-------|-------|--------------|-------|--------------|
| | | Va. | Dis. | Al. | Ep. | En. | Va. | Dis. | Al. | Ep. | En. | |
| Mov-Sim | Dropout | - | - | 69.55 | 69.67 | 72.64 | - | - | 29.61 | 34.71 | 32.62 | 83.94 |
| | PN | 81.73 | 53.41 | 65.60 | 81.73 | 63.73 | 43.25 | 17.47 | 30.20 | 43.25 | 26.94 | 82.43 |
| | E-NER | 84.20 | 60.47 | 84.10 | 84.20 | 84.02 | 41.44 | 19.92 | 39.97 | 41.44 | 39.95 | 70.63 |
| | SLPN(w/o softplus) | 55.37 | 31.44 | 36.33 | 55.37 | 26.81 | 23.33 | 12.96 | 15.99 | 23.33 | 12.63 | 66.95 |
| | Ours(SLPN) | 81.29 | 53.59 | 64.10 | 81.29 | 61.27 | 50.31 | 17.56 | 30.77 | 50.31 | 25.57 | 83.37 |
| MIT-Res | Dropout | - | - | 58.01 | 64.26 | 61.08 | - | - | 39.97 | 54.36 | 45.52 | 74.60 |
| | PN | 73.50 | 69.44 | 60.98 | 73.50 | 70.03 | 53.39 | 45.16 | 43.07 | 53.39 | 47.88 | 74.37 |
| | E-NER | 76.67 | 75.76 | 74.53 | 76.67 | 75.76 | 51.27 | 49.79 | 49.11 | 51.27 | 49.79 | 69.08 |
| | SLPN(w/o softplus) | 44.30 | 43.92 | 46.22 | 44.30 | 41.69 | 32.66 | 33.74 | 33.78 | 32.66 | 31.41 | 62.16 |
| | Ours(SLPN) | 75.13 | 45.76 | 54.85 | 75.13 | 50.96 | 58.93 | 35.63 | 38.73 | 58.93 | 38.62 | 74.65 |
| Mov-Com | Dropout | - | - | 50.38 | 50.75 | 50.74 | - | - | 12.33 | 14.27 | 12.52 | 72.51 |
| | PN | 75.81 | 68.86 | 72.43 | 75.81 | 70.59 | 25.47 | 18.85 | 23.92 | 25.47 | 21.65 | 70.13 |
| | E-NER | 86.43 | 79.90 | 85.41 | 86.43 | 82.65 | 39.83 | 26.54 | 32.57 | 39.83 | 30.52 | 67.21 |
| | SLPN(w/o softplus) | 59.59 | 50.07 | 53.81 | 59.59 | 50.47 | 18.71 | 12.60 | 16.90 | 18.71 | 13.94 | 66.05 |
| | Ours(SLPN) | 87.39 | 44.28 | 71.63 | 87.39 | 55.35 | 39.85 | 12.47 | 21.41 | 39.85 | 15.24 | 70.97 |

Table 5: Uncertainty estimation results on WS task. The usage of bold font is the same as Table 2.

| Data | Model | AUROC on WS task | | | | | AUPR on WS task | | | | | F1 |
|---------|--------------------|------------------|-------|--------------|--------------|-------|-----------------|-------|-------|--------------|--------------|--------------|
| | | Va. | Dis. | Al. | Ep. | En. | Va. | Dis. | Al. | Ep. | En. | |
| Mov-Sim | Dropout | - | - | 63.12 | 79.96 | 68.82 | - | - | 17.81 | 30.02 | 22.86 | 83.94 |
| | PN | 66.43 | 59.83 | 71.76 | 66.43 | 72.74 | 28.11 | 13.82 | 30.66 | 28.11 | 31.91 | 82.43 |
| | E-NER | 58.47 | 54.96 | 55.81 | 58.47 | 59.11 | 21.83 | 21.95 | 23.44 | 21.83 | 24.80 | 70.63 |
| | SLPN(w/o softplus) | 71.92 | 60.10 | 67.79 | 71.92 | 63.51 | 42.11 | 25.55 | 42.07 | 42.11 | 36.11 | 66.95 |
| | Ours(SLPN) | 60.60 | 58.09 | 66.26 | 60.60 | 67.87 | 28.43 | 13.07 | 28.34 | 28.43 | 30.11 | 83.37 |
| MIT-Res | Dropout | - | - | 72.32 | 71.70 | 71.54 | - | - | 24.61 | 24.39 | 25.28 | 74.60 |
| | PN | 56.25 | 56.40 | 65.63 | 56.25 | 56.18 | 21.84 | 18.24 | 22.93 | 21.84 | 20.87 | 74.37 |
| | E-NER | 40.25 | 41.21 | 38.21 | 40.25 | 41.27 | 11.94 | 12.22 | 11.61 | 11.94 | 12.24 | 69.08 |
| | SLPN(w/o softplus) | 64.43 | 62.97 | 65.66 | 64.43 | 67.27 | 33.62 | 27.16 | 32.68 | 33.62 | 34.39 | 62.16 |
| | Ours(SLPN) | 51.34 | 61.44 | 65.61 | 51.34 | 60.52 | 17.04 | 19.16 | 22.46 | 17.04 | 21.10 | 74.65 |
| Mov-Com | Dropout | - | - | 72.06 | 73.41 | 72.20 | - | - | 30.96 | 31.82 | 31.97 | 72.51 |
| | PN | 64.98 | 66.17 | 67.82 | 64.98 | 66.63 | 37.13 | 32.81 | 36.07 | 37.13 | 36.50 | 70.13 |
| | E-NER | 57.92 | 59.35 | 59.48 | 57.92 | 58.86 | 21.37 | 22.51 | 22.21 | 21.37 | 22.03 | 67.21 |
| | SLPN(w/o softplus) | 63.10 | 63.07 | 66.00 | 63.10 | 65.63 | 37.96 | 37.39 | 38.97 | 37.96 | 40.03 | 66.05 |
| | Ours(SLPN) | 66.05 | 59.16 | 70.04 | 66.05 | 61.52 | 35.00 | 30.12 | 35.88 | 35.00 | 34.41 | 70.97 |

make the model performs in a stable way. When we remove the softplus operation (SLPN w/o softplus) and compare it with SLPN, we observe a significant performance decrease in both UE-NER and NER tasks. Table 2 indicates that NER F1 scores drop by over 10 points in both datasets, while UE-NER AUROC and AUPR scores decrease by more than 15 points. Thus, it is crucial to design the softplus operation in Eq. 8 to ensure β_i^{trans} remains positive.

7 Conclusion

Incorrect NER predictions incur significant penalties. We primarily focus on UE-NER, which differs from prior uncertainty estimation methods that focus on sample-level labeling. UE-NER centers on token-level sequential labeling, addressing the overlooked transmitted uncertainty from contextual tokens. We introduce SLPN to calculate uncertainty from both the token itself and contextual tokens, enhancing OOD detection in NER. Additionally, for OOD detection in NER, WS entities are not applicable. Thus, we divide the entities into two distinct subsets—one for OOD detection and the other for WS detection. Our experiments validate

SLPN’s effectiveness and the importance of considering uncertainty propagation in UE-NER.

8 Ethical Considerations

This study pioneers uncertainty estimation in sequential labeling, specifically in the context of Named Entity Recognition (NER). Additionally, we have innovatively proposed to account for uncertainty transmission, which is ignored in sample-level classification.

Our research exclusively employs datasets that are publicly available, ensuring transparency and accessibility. Our usage of Flair and related datasets obey their MIT licenses.

9 Limitations

This paper introduces SLPN for uncertainty estimation in sequential labeling. However, SLPN exhibits two main limitations: First, it is based on the Posterior Network, and we plan to assess its generalization capabilities across other models. Second, our implementation of SLPN does not treat sequential labeling as a generative task, which would be meaningful to explore, especially in considering uncertainty propagation in generative tasks.

References

Alan Akbik, Tanja Bergmann, Duncan Blythe, Kashif Rasul, Stefan Schweter, and Roland Vollgraf. 2019. FLAIR: An easy-to-use framework for state-of-the-art NLP. In *NAACL 2019, 2019 Annual Conference of the North American Chapter of the Association for Computational Linguistics (Demonstrations)*, pages 54–59.

Alexander Amini, Wilko Schwarting, Ava Soleimany, and Daniela Rus. 2020. Deep evidential regression. *Advances in Neural Information Processing Systems*, 33:14927–14937.

Haw-Shiuan Chang, Shankar Vembu, Sunil Mohan, Rheeyaa Uppaal, and Andrew McCallum. 2020. Using error decay prediction to overcome practical issues of deep active learning for named entity recognition. *Machine Learning*, 109:1749–1778.

Bertrand Charpentier, Daniel Zügner, and Stephan Günnemann. 2020. Posterior network: Uncertainty estimation without ood samples via density-based pseudo-counts. *Advances in Neural Information Processing Systems*, 33:1356–1367.

Jason PC Chiu and Eric Nichols. 2016. Named entity recognition with bidirectional lstm-cnns. *Transactions of the association for computational linguistics*, 4:357–370.

Jacob Devlin, Ming-Wei Chang, Kenton Lee, and Kristina Toutanova. 2018. Bert: Pre-training of deep bidirectional transformers for language understanding. *arXiv preprint arXiv:1810.04805*.

Bo Dong, Yiyi Wang, Hanbo Sun, Yunji Wang, Alireza Hashemi, and Zheng Du. 2022a. Cml: A contrastive meta learning method to estimate human label confidence scores and reduce data collection cost. In *Proceedings of The Fifth Workshop on e-Commerce and NLP (ECNLP 5)*, pages 35–43.

Bo Dong, Yuhang Wu, Micheal Yeh, Yusan Lin, Yuzhong Chen, Hao Yang, Fei Wang, Wanxin Bai, Krupa Brahmstrik, Zhang Yimin, et al. 2022b. Semi-supervised context discovery for peer-based anomaly detection in multi-layer networks. In *Information and Communications Security: 24th International Conference, ICICS 2022, Canterbury, UK, September 5–8, 2022, Proceedings*, pages 508–524. Springer.

Luciano Floridi and Massimo Chiriatti. 2020. Gpt-3: Its nature, scope, limits, and consequences. *Minds and Machines*, 30:681–694.

Yarin Gal and Zoubin Ghahramani. 2016. Dropout as a bayesian approximation: Representing model uncertainty in deep learning. In *international conference on machine learning*, pages 1050–1059.

James Hammerton. 2003. Named entity recognition with long short-term memory. In *Proceedings of the seventh conference on Natural language learning at HLT-NAACL 2003*, pages 172–175.

Russell Alan Hart, Linlin Yu, Yifei Lou, and Feng Chen. 2023. Improvements on uncertainty quantification for node classification via distance-based regularization.

Jianfeng He, Hang Su, Jason Cai, Igor Shalyminov, Hwanjun Song, and Saab Mansour. 2024. Semi-supervised dialogue abstractive summarization via high-quality pseudolabel selection. *arXiv preprint arXiv:2403.04073*.

Jianfeng He, Xuchao Zhang, Shuo Lei, Zhiqian Chen, Fanglan Chen, Abdulaziz Alhamadani, Bei Xiao, and ChangTien Lu. 2020. Towards more accurate uncertainty estimation in text classification. In *Proceedings of the 2020 Conference on Empirical Methods in Natural Language Processing (EMNLP)*, pages 8362–8372.

Dan Hendrycks and Kevin Gimpel. 2016. A baseline for detecting misclassified and out-of-distribution examples in neural networks. *arXiv preprint arXiv:1610.02136*.

Yibo Hu and Latifur Khan. 2021. Uncertainty-aware reliable text classification. In *Proceedings of the 27th ACM SIGKDD Conference on Knowledge Discovery & Data Mining*, pages 628–636.

Zhiheng Huang, Wei Xu, and Kai Yu. 2015. Bidirectional lstm-crf models for sequence tagging. *arXiv preprint arXiv:1508.01991*.

Audun Jøsang. 2018. *Subjective Logic: A formalism for reasoning under uncertainty*. Springer Publishing Company, Incorporated.

Guillaume Lample, Miguel Ballesteros, Sandeep Subramanian, Kazuya Kawakami, and Chris Dyer. 2016. Neural architectures for named entity recognition. *arXiv preprint arXiv:1603.01360*.

Shuo Lei, Xuchao Zhang, Jianfeng He, Fanglan Chen, and Chang-Tien Lu. 2022. Uncertainty-aware cross-lingual transfer with pseudo partial labels. In *Findings of the Association for Computational Linguistics: NAACL 2022*, pages 1987–1997.

Jeremiah Liu, Zi Lin, Shreyas Padhy, Dustin Tran, Tania Bedrax Weiss, and Balaji Lakshminarayanan. 2020. Simple and principled uncertainty estimation with deterministic deep learning via distance awareness. In *Advances in Neural Information Processing Systems*, volume 33, pages 7498–7512. Curran Associates, Inc.

Mingyi Liu, Zhiying Tu, Tong Zhang, Tonghua Su, Xiaofei Xu, and Zhongjie Wang. 2022. Ltp: A new active learning strategy for crf-based named entity recognition. *Neural Processing Letters*, 54(3):2433–2454.

Wesley J Maddox, Pavel Izmailov, Timur Garipov, Dmitry P Vetrov, and Andrew Gordon Wilson. 2019. A simple baseline for bayesian uncertainty in deep learning. *Advances in Neural Information Processing Systems*, 32.

Andrey Malinin and Mark Gales. 2018. Predictive uncertainty estimation via prior networks. *Advances in neural information processing systems*, 31.

Larry R Medsker and LC Jain. 2001. Recurrent neural networks. *Design and Applications*, 5(64-67):2.

Shervin Minaee, Nal Kalchbrenner, Erik Cambria, Narjes Nikzad, Meysam Chenaghlu, and Jianfeng Gao. 2021. Deep learning-based text classification: a comprehensive review. *ACM computing surveys (CSUR)*, 54(3):1–40.

Jishnu Mukhoti, Andreas Kirsch, Joost van Amersfoort, Philip HS Torr, and Yarin Gal. 2023. Deep deterministic uncertainty: A new simple baseline. In *Proceedings of the IEEE/CVF Conference on Computer Vision and Pattern Recognition*, pages 24384–24394.

Minh-Tien Nguyen, Guido Zuccon, Gianluca Demartini, et al. 2021. Loss-based active learning for named entity recognition. In *2021 International Joint Conference on Neural Networks (IJCNN)*, pages 1–8. IEEE.

Kazuki Osawa, Siddharth Swaroop, Mohammad Emtiyaz E Khan, Anirudh Jain, Runa Eschenhagen, Richard E Turner, and Rio Yokota. 2019. Practical deep learning with bayesian principles. *Advances in neural information processing systems*, 32.

Sungrae Park, JunKeon Park, Su-Jin Shin, and Il-Chul Moon. 2018. Adversarial dropout for supervised and semi-supervised learning. In *Thirty-Second AAAI Conference on Artificial Intelligence*.

Danilo Rezende and Shakir Mohamed. 2015. Variational inference with normalizing flows. In *International conference on machine learning*, pages 1530–1538. PMLR.

Murat Sensoy, Lance Kaplan, and Melih Kandemir. 2018. Evidential deep learning to quantify classification uncertainty. *Advances in neural information processing systems*, 31.

Maximilian Stadler, Bertrand Charpentier, Simon Geisler, Daniel Zügner, and Stephan Günnemann. 2021. Graph posterior network: Bayesian predictive uncertainty for node classification. *Advances in Neural Information Processing Systems*, 34.

Kelei Sun, Jiaming Yu, Li Zhang, and Zhiheng Dong. 2020. A convolutional neural network model based on improved softplus activation function. In *International Conference on Applications and Techniques in Cyber Intelligence ATCI 2019: Applications and Techniques in Cyber Intelligence 7*, pages 1326–1335. Springer.

Ashish Vaswani, Noam Shazeer, Niki Parmar, Jakob Uszkoreit, Llion Jones, Aidan N Gomez, Łukasz Kaiser, and Illia Polosukhin. 2017. Attention is all you need. *Advances in neural information processing systems*, 30.

Artem Vazhentsev, Gleb Kuzmin, Artem Shelmanov, Akim Tsvigun, Evgenii Tsymbalov, Kirill Fedyanin, Maxim Panov, Alexander Panchenko, Gleb Gusev, Mikhail Burtsev, et al. 2022. Uncertainty estimation of transformer predictions for misclassification detection. In *Proceedings of the 60th Annual Meeting of the Association for Computational Linguistics (Volume 1: Long Papers)*, pages 8237–8252.

Dingrong Wang, Deep Shankar Pandey, Krishna Prasad Neupane, Zhiwei Yu, Ervine Zheng, Zhi Zheng, and Qi Yu. 2023a. Deep temporal sets with evidential reinforced attentions for unique behavioral pattern discovery. In *International Conference on Machine Learning*, pages 36205–36223. PMLR.

Shuhe Wang, Xiaofei Sun, Xiaoya Li, Rongbin Ouyang, Fei Wu, Tianwei Zhang, Jiwei Li, and Guoyin Wang. 2023b. Gpt-ner: Named entity recognition via large language models. *arXiv preprint arXiv:2304.10428*.

Yaqing Wang, Subhabrata Mukherjee, Haoda Chu, Yuancheng Tu, Ming Wu, Jing Gao, and Ahmed Hassan Awadallah. 2021. Meta self-training for few-shot neural sequence labeling. In *Proceedings of the 27th ACM SIGKDD Conference on Knowledge Discovery & Data Mining*, pages 1737–1747.

Linlin Yu, Yifei Lou, and Feng Chen. 2023. Uncertainty-aware graph-based hyperspectral image classification. In *The Twelfth International Conference on Learning Representations*.

Xuchao Zhang, Fanglan Chen, Chang-Tien Lu, and Naren Ramakrishnan. 2019. Mitigating uncertainty in document classification. In *Proceedings of NAACL-HLT*, pages 3126–3136.

Zhen Zhang, Mengting Hu, Shiwan Zhao, Minlie Huang, Haotian Wang, Lemao Liu, Zhirui Zhang, Zhe Liu, and Bingzhe Wu. 2023. E-ner: Evidential deep learning for trustworthy named entity recognition. *arXiv preprint arXiv:2305.17854*.

Xujiang Zhao, Feng Chen, Shu Hu, and Jin-Hee Cho. 2020. Uncertainty aware semi-supervised learning on graph data. *Advances in Neural Information Processing Systems*, 33:12827–12836.

A Appendix

A.1 Model

A.1.1 Explanation of Softplus

Since evidential learning is an evidence acquisition process, which means that every token in a training text contributes to learning an evidence matrix ($\beta^{trans,t}$) (Wang et al., 2023a; Sensoy et al., 2018; Amini et al., 2020), we expect that $\beta^{trans,t}$ has all elements (e.g., all tokens’ evidence in the respective class) greater than 0. Therefore, we expect every element of the evidential matrix ($\beta^{trans,t}$) to be greater than 0.

Based on Eq 9, we understand that $\beta^{trans,t}$ consists of two parts: the softmax part and V . If we expect $\beta^{trans,t}$ to be greater than 0, the only potential negative case might be from V . Consequently, we anticipate that V is greater than 0. Therefore, we choose the Softplus function, which is defined as follows:

$$Softplus(x) = \log(1 + e^x). \quad (13)$$

Considering the formula of Softplus, it is always greater than 0. In addition to ensuring V is greater than 0 in Eq 8, we opt for Softplus as it helps prevent gradient explosion and gradient vanishing issues due to its smooth transition between the positive and negative parts of the input.

A.2 Experiments

A.2.1 Criteria of Dataset Choice

We select the dataset based on two criteria: firstly, the dataset should contribute to reproducibility, and secondly, the dataset should not have an F1 score higher than 90%. We prioritize high reproducibility because we aim for our work to be replicable by others. We do not anticipate achieving an F1 score higher than 90%, as this would suggest that the dataset has already been thoroughly studied or that the model’s uncertainty for that dataset is relatively low.

To meet the reproducibility criterion, we utilize the dataset provided by the Flair framework (Akbik et al., 2019). In adherence to the second criterion, we exclude CONLL_03 dataset from consideration due to its 94% F1 score in NER task. From the datasets listed in Flair framework (Akbik et al., 2019), we randomly select two domains: the restaurant domain and the movie domain. For the restaurant domain, we opt for the MIT-Restaurant dataset. In the movie domain, Flair offers both a

simple movie dataset and a complex movie dataset. We are interested in investigating whether there exists a tradeoff between uncertainty scores and F1 scores in UE-NER. Consequently, we select the simple-movie dataset and the complex-movie dataset, which exhibit higher and lower NER performance, as measured by the F1 score, in UE-NER, respectively. As for the tradeoff, after excluding the impact of different domains, we do not observe a significant tradeoff between the quality of uncertainty estimation (measured by AUROC) and NER task performance (measured by F1 score) when comparing the same method’s AUROC and F1 between Mov-Sim and Mov-Com.

A.2.2 Reason of Entity-Level Evaluation

We choose entity-level evaluation instead of token level because it has more practical applications and is more commonly used in other NER works than token-level evaluation (e.g., “New” is a token with a label “b-LOC,” and “York” is a token with a label “e-LOC”). Classifying “New” correctly and “York” incorrectly cannot lead to our desired correct entity.

A.2.3 Metrics

Below, we introduce the formulas used for the five metrics. Given a prediction from an EDL model, i.e., α , we have the total evidence $\alpha_0 = \sum_{k=1}^c \alpha_k$ (as in Eq.2) where c is the number of classes. The expected class probability is $\bar{p} = \frac{\alpha}{\alpha_0}$.

From the evidential view, we have dissonance and vacuity uncertainty for EDL-based models. The dissonance uncertainty in EDL is calculated via Eq. 5 in Zhao et al. (2020).

$$u^{\text{diss}} = \sum_{k=1}^c \frac{b_k \sum_{j \neq k} b_j \text{Bal}(b_j, b_k)}{\sum_{j \neq k} b_j} \quad (14)$$

with $b_k = \frac{\alpha_k - 1}{\alpha_0}$ and $\text{Bal}(b_j, b_k) = 1 - \frac{|b_j - b_k|}{b_j + b_k}$. It measures the uncertainty due to the conflicting evidence. The vacuity uncertainty in EDL is related to α_0 in Eq.2, which represents the total evidence,

$$u^{\text{vac}} = \frac{c}{\alpha_0} \quad (15)$$

From a probabilistic view, we have aleatoric uncertainty and epistemic uncertainty. The aleatoric uncertainty is calculated based on the projected or expected class probabilities,

$$u^{\text{alea}} = \frac{1}{\max_k \bar{p}_k} \quad (16)$$

The epistemic uncertainty is calculated based on total evidence in EDL-based models,

$$u^{\text{epis}} = \frac{1}{\alpha_0} \quad (17)$$

Because our vacuity uncertainty and epistemic uncertainty calculation are based on α_0 and are similar, they have the same sample rank regarding uncertainty score.

For dropout models, where the aleatoric and epistemic uncertainty are calculated from a probabilistic view, please refer to [He et al. \(2024\)](#); [Mukhoti et al. \(2023\)](#).

We also report the entropy as the uncertainty score, which is calculated with the expected categorical distribution.

$$u^{\text{entropy}} = \mathbb{H}(\bar{\mathbf{p}}) \quad (18)$$